Interaction of silver nanoparticles with metallothionein and ceruloplasmin: impact on metal substitution by Ag(I), corona formation and enzymatic activity

Wei Liu, Isabelle A.M. Worms, Nathalie Herlin-Boime, Delphine Boutry-Truffier, Isabelle Michaud-Soret, Elisabeth Mintz, Claude Vidaud, Françoise Rollin-Genetet

Table S1 — Operating conditions for fractionation and detection of MT1, Cp and their metal content

	MT1	**Cp**
Fractionation		
Spacer	490 µm	350 µm
Membrane	1 kDa RC[a] (Postnova analytic)	10 kDa RC (Superon)
Detector Flow	DF[b] = 1 mL min^{-1}	DF = 1 mL min^{-1}
Elution	XF[c] = 1.5 mL min^{-1}; 2 min	XF = 2 mL min^{-1}; 2 min
Focus	XF = 1.5 mL min^{-1}; 1 min	XF = 2 mL min^{-1}; 1 min
Focus and injection	XF = 1.5 mL min^{-1}; InjF[d] = 0.2 mL min^{-1}; 5min	XF = 2 mL min^{-1} InjF = 0.2 mL min^{-1}; 5 min
Focus	XF = 1.5 mL min^{-1}; 1 min	XF = 2 mL min^{-1}; 1 min
Elution	Cte XF = 1.5 mL min^{-1}; 10 min	Cte XF = 2 mL min^{-1}; 1 min; Grad XF = 2-0.1 mL min^{-1}; 20 min
Post-Elution wash	XF = 1.5-0 mL min^{-1}; 5 min	XF = 0 mL min^{-1}; 5 min
Elution and injection wash	XF = 0 mL min^{-1}; InjF = 0.2 mL min^{-1}; 5 min	XF = 0 mL min^{-1}; InjF = 0.2 mL min^{-1}; 5 min
Detection		
UV wavelength	245 nm	280 nm
Recovery (%)	70 ± 8	85.5 ± 0.5
ICP-MS operating conditions	Normal mode (Ar); RF power = 1550 W; Sampling depth = 7.5 mm; TRA; acquisition time/mass = 1 s	
Isotopes	^{107}Ag ^{111}Cd ^{114}Cd ^{66}Zn	^{107}Ag ^{63}Cu ^{65}Cu
Peristaltic pump rotation	0.1 rpm	

[a] RC = regenerated cellulose; [b] DF = detector flow rate; [c] XF = cross flow rate (either constant (Cte) or Gradient exponential decrease (Grad); [d] InjF = injection flow rate

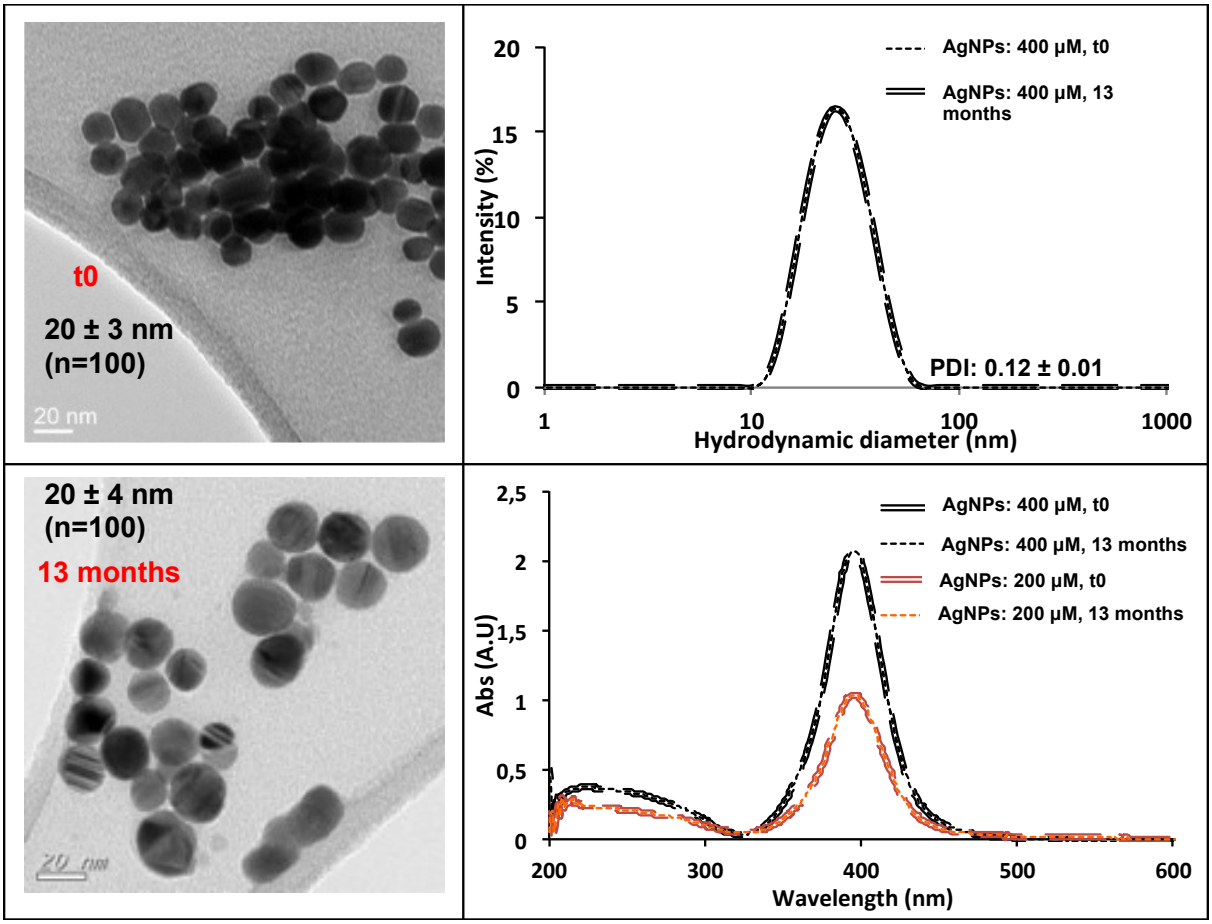

Fig. S1 TEM image, DLS evaluation of the hydrodynamic diameter distribution (expressed in % of intensity) and UV-visible spectra of AgNPs at first preparation (t0) and 13 months later.

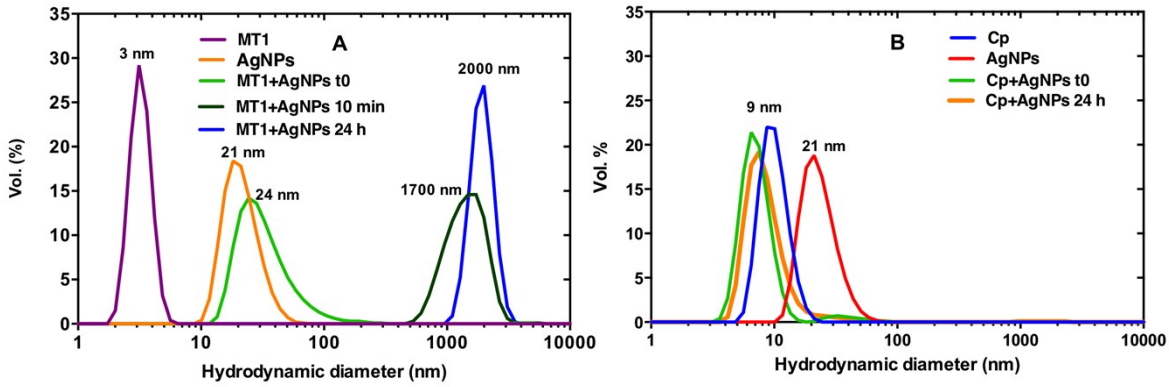

Fig. S2 DLS evaluation of the hydrodynamic diameter distribution (in % of volume) in various suspensions; AgNPs (orange), proteins (purple) and AgNP-protein mixtures at different time-points, t0 (light green), 10 min (dark green), 24 h (blue). (A): 600 µM AgNPs and/or 150 µM MT1 (4 Ag eq. per MT1); (B): 30 µM AgNPs and/or 5 µM Cp (6 Ag eq. per Cp).

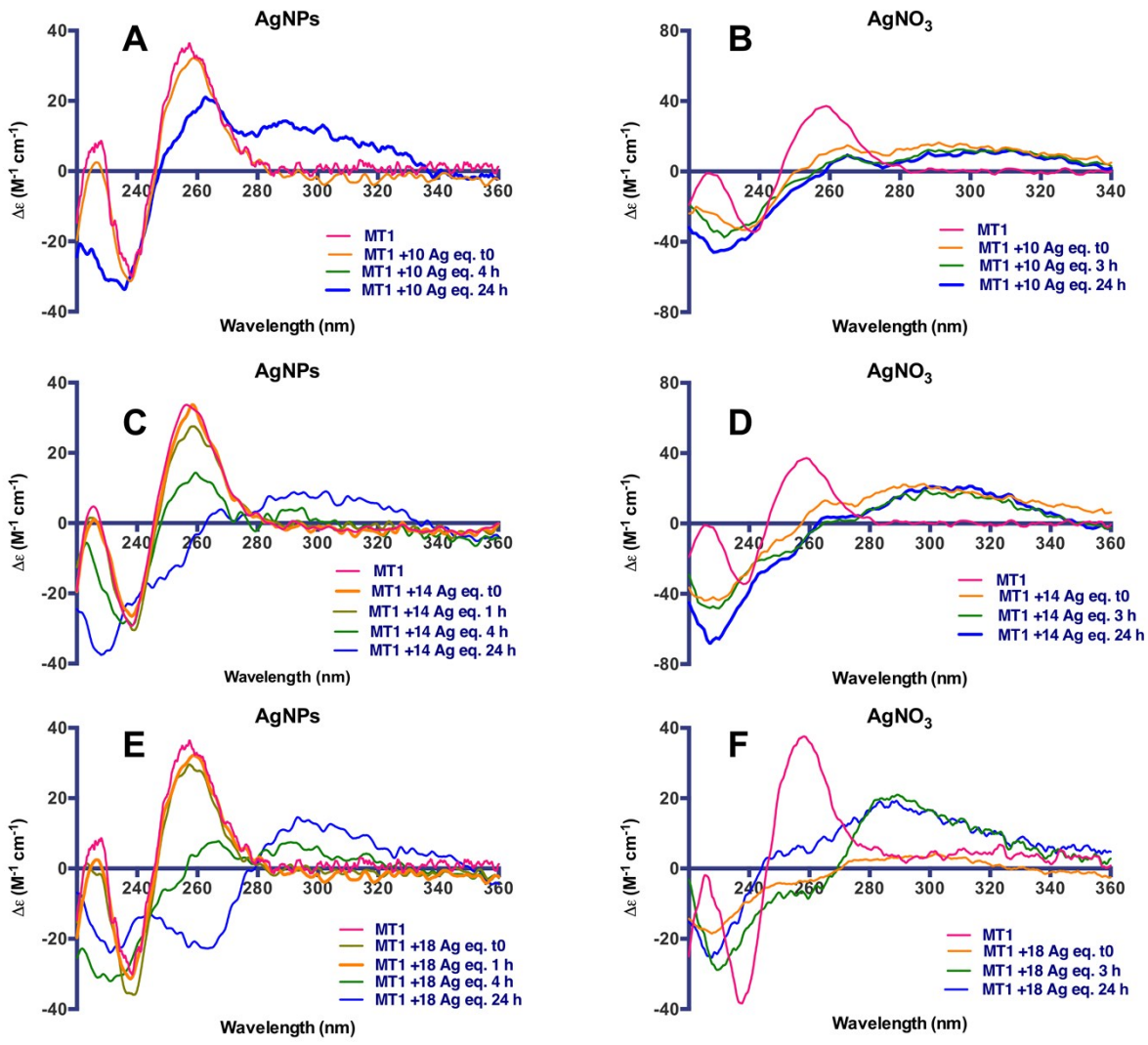

Fig. S3 CD spectra evolutions versus time and expressed in $\Delta\varepsilon$ (M^{-1} cm^{-1}) for 20 µM MT1 mixed with varied amounts (from 10 to 18 Ag eq.) of AgNPs or $AgNO_3$.

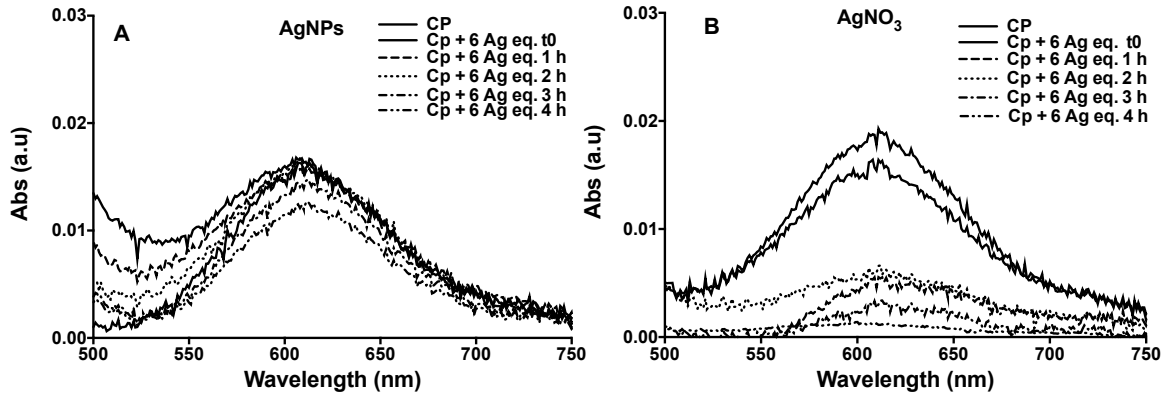

Fig. S4 Evolution of the blue copper-site absorption band versus time followed by UV Visible spectroscopy of Cp in the presence of AgNPs (A) or $AgNO_3$ (B), with 15 µM Cp and 6 Ag eq. (90 µM).

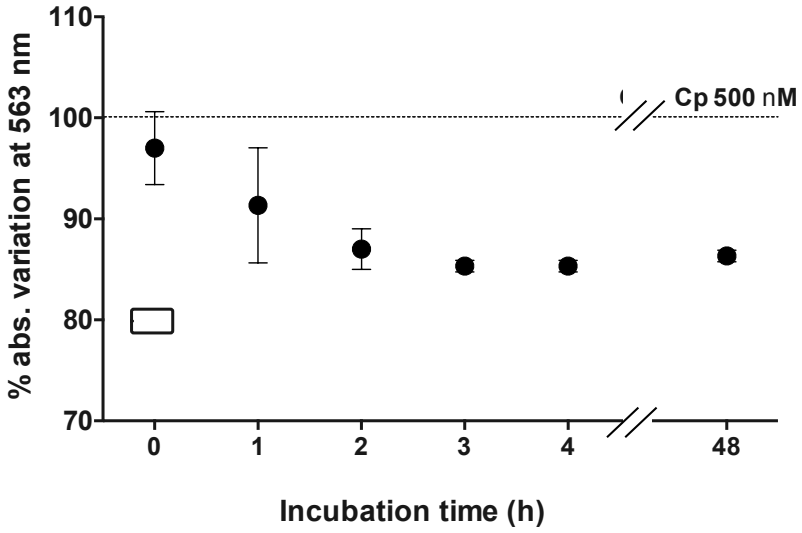

Fig. S5 Evolution of the ferroxidase activity of Cp (500 nM) mixed with 6 Ag eq. as AgNPs (■). The activity was evaluated as the absorbance variations (in %) at 563 nm versus time and normalized to the Cp signal (dotted line) for the formation of the ferrous-ferrozine complex. The instantaneous inhibition of the ferroxidase activity by $AgNO_3$ (□) has been used as reference level.

Supplementary information related to AF4-UVD-ICP-MS

SI.1. Metal Quantification

Metal quantification was performed using an external calibration obtained by 10 to 50 µL injections of individual standard suspensions of AgNPs and solutions of MT1 and Cp prepared in HEPES-citrate buffer, after replacing the AF4 channel by a 3 ways connector. Following the direct injection elution at DF = 1 mL min^{-1} and InjF = 0.2 mL min^{-1} using the same buffer as used for AF4 elution (10 mM HEPES pH 7.1), signals were recorded over 15 min (Fig. S6A, C, E, G), CPS peaks were integrated over time and the area was related to the mass of injected metals. The linear relationship $Area = f(m_{injected})$ was used to quantify the metal recovered for each analysis (Fig. S6B, D, F, H). Total metal content of each standard was quantified by ICP-MS after dilution, either in the mobile phase or under acidic conditions (1% HNO_3) when appropriate.

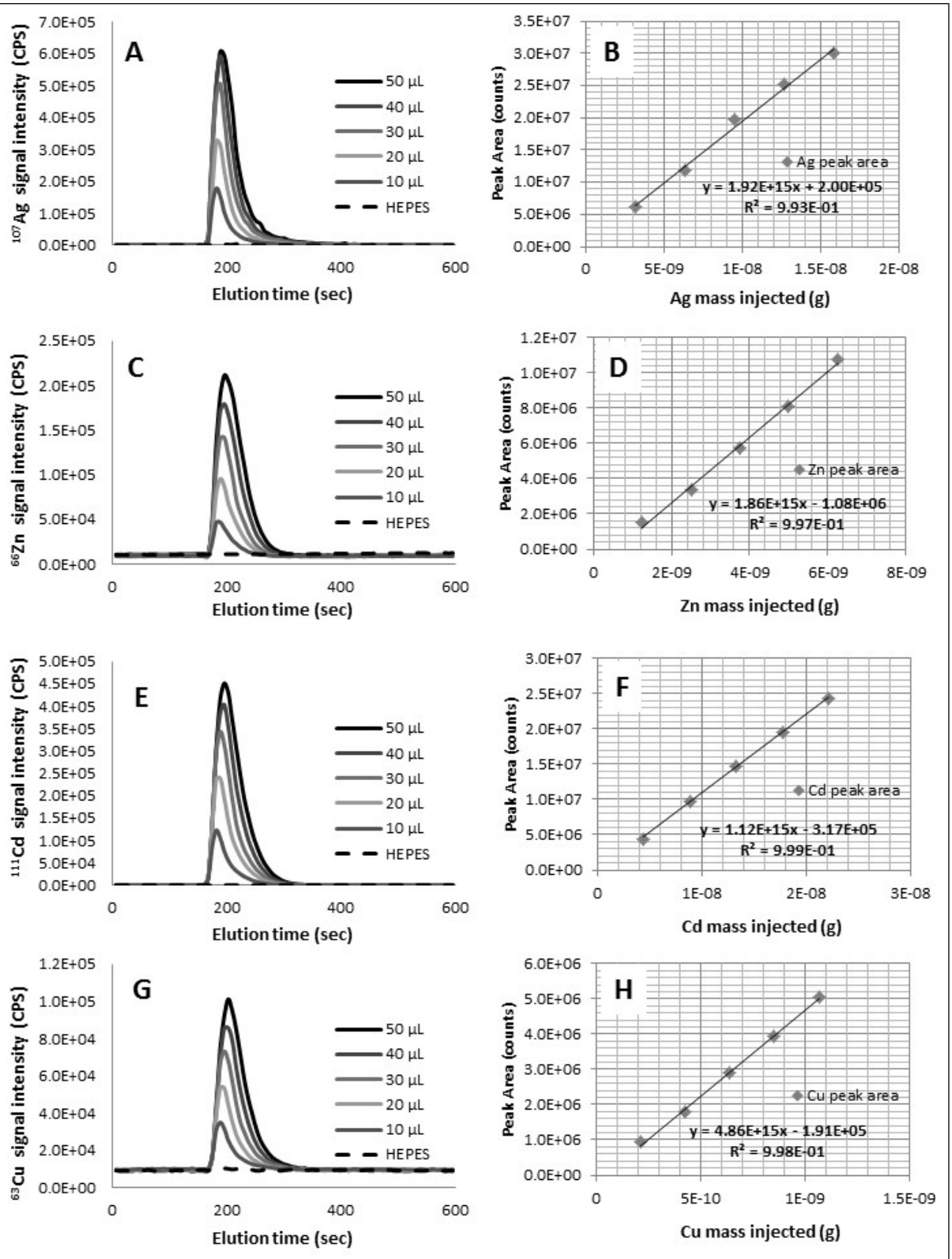

Fig. S6 External calibration of ICP-MS signal. Direct injection (without channel) of individual standard samples of 318 ppb AgNPs (20 nm), 444 ppb Cd-, 125 ppb Zn-MT1 or 21.4 ppb Cu-Cp. ICP-MS fractograms obtained for 10 to 50 µL injections (A; ^{107}Ag for AgNPs), (C; ^{66}Zn for Zn-MT1), (E; ^{111}Cd for Cd-MT1), (G; ^{63}Cu for Cu-Cp). A 50 µL injection of HEPES-citrate buffer was performed at the end of each serial injection to check for residual contamination of the injection loop. Calibration curves B, D, F and H were obtained using peak integration of the fractograms A, C, E and G respectively.

SI.2. Optimization of the elution conditions for MT1

In the case of AgNP-MT1, the elution of AgNPs was not possible while using 10 mM HEPES pH 7.1, a mobile phase close to the buffer used for AgNP-protein interaction studies. Using 0.1 mM NaOH (pH 10) as mobile phase and a lower XF, nano-objects were however transiently identified (Fig. S7)

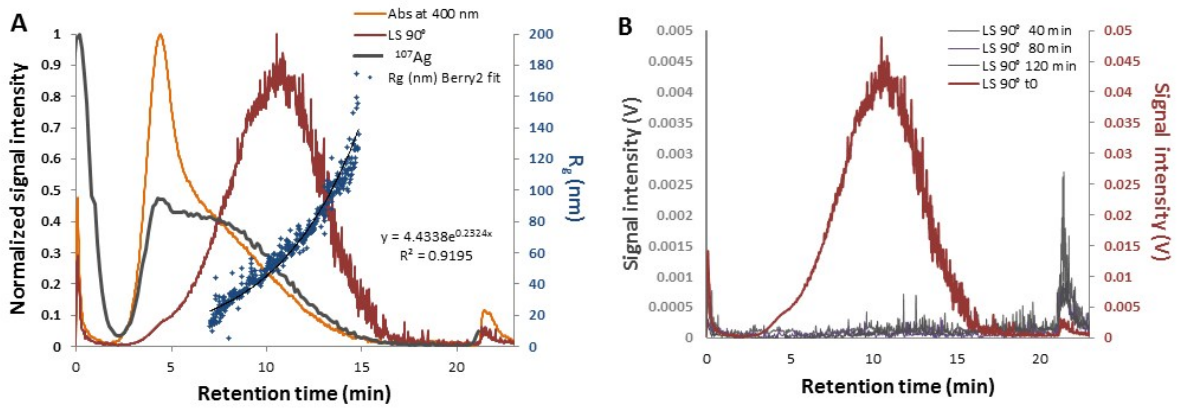

Fig. S7 Identification of AgNPs aggregation due to the addition of MT1. (A) Fractograms obtained using UVD at 400 nm (orange line), light scattered recorded at 90° angle detector of MALLS (LS 90°, red line) and ^{107}Ag isotope recorded by ICP-MS (grey line) for AgNP-MT1 sample at t0. Data obtained for MALLS were integrated to obtain gyration radius values (R_g, blue dots) using the Berry 2 model in ASTRA software (Wyatt technology). (B) Fractograms obtained following LS 90° for 11 Ag eq. AgNPs incubated for t0 (red line), 40, 80 or 120 min (grey lines) with 20 µM MT1 in HEPES-citrate buffer. All the samples were analyzed following a 10-fold dilution in the mobile phase (0.1 mM NaOH pH 10). t0 corresponded to immediate mixing and dilution of AgNPs suspension with MT1. (V_{inj} =50 µL; 350 µm spacer; 10 kDa membrane; XF = 1-0 mL min^{-1}; 0.1 mM NaOH pH 10 as mobile phase).

At t0, the fractogram of silver species distribution showed a higher polydispersity with increased retention times as compared to AgNPs (t_{rAgNPs} = 3.7 min, Fig. S7A). In order to determine the size distribution parameters of these AgNP-MT1 aggregates, the relationship between gyration radius (R_g), obtained by Berry 2 data treatment of scattered light, and the retention time was derived. A ~ 52 nm average diameter ($d_{g,n}$, expressed in number) and a ~ 67 nm weighted average diameter ($d_{g,w}$) were estimated from ICP-MS fractogram, those values being in agreement with the ~ 50 nm hydrodynamic diameter (d_H) measured in the batch suspensions by DLS. Thereafter, the aggregates could not be eluted under similar

elution conditions, as illustrated by the back to noise level of the scattered light when AgNPs were incubated with MT1 for 40, 80 and 120 min (Fig. S7B). This could easily be explained by the micrometer size of the objects identified by DLS at those interaction times, which cannot be eluted under the operating conditions used here. Most of all, no increase of LS signal compared to the t0 injection was recorded when the cross-flow was decreased up to 0 mL min^{-1} at the end of the run, indicating that the aggregates should certainly be adsorbed on the membrane.

When using 10 mM HEPES pH 7.1 as mobile phase, the transient small sized aggregates formed at t0 were not eluted. However, this mobile phase was chosen in order to minimize the pH and the ionic strength effects on the MT1 stoichiometry.

In order to gain in the separation efficiency of this small 7 kDa protein, a 490 µm spacer was used together with a decreased in XF strength during elution, a factor that affected the MT1 recovery when the 350 µm spacer was used (data not shown). For all the experiments, the UV detector was set at 245 nm because MT1 lacks aromatic residues and because the absorbance intensity at this wavelength was remarkably stable in batch experiments, whatever the incubation conditions (see UV-visible and CD spectra).

An optimum cross-flow of 1.5 mL min^{-1} was chosen leading to a protein channel recovery of R = 70 ± 8 % compared to direct injection-elution in the channel (InjF = 0.2 mL min^{-1}, XF = 0 mL min^{-1}, DF = 1 mL min^{-1} over 15 min). This pre-optimization was carried out by comparing the recovered absorbance at 245 nm under fractionation conditions to those obtained in the absence of cross-flow (direct injection in the channel, InjF = 0.2 mL min^{-1}, XF = 0 mL min^{-1}, DF = 1 mL min^{-1} over 15 min), a methodology which is commonly applied but which did not account for global system artifacts.[1] Indeed, these results were also compared to direct injection of the samples in a 3 ways connector replacing the AF4 channel (build-up similar to that used to perform external calibration SI.1). Using the 3 ways connector had no

effect on signal area compared to XF = 0 mL min^{-1} procedure, meaning that a protein loss certainly occurred during the injection step, probably due to interaction of proteins with the membrane. Despite such artifact, the quantity of recovered protein was evaluated for each run using a linear calibration curve that accounted for this protein loss (depicted in the inset Fig. S8).

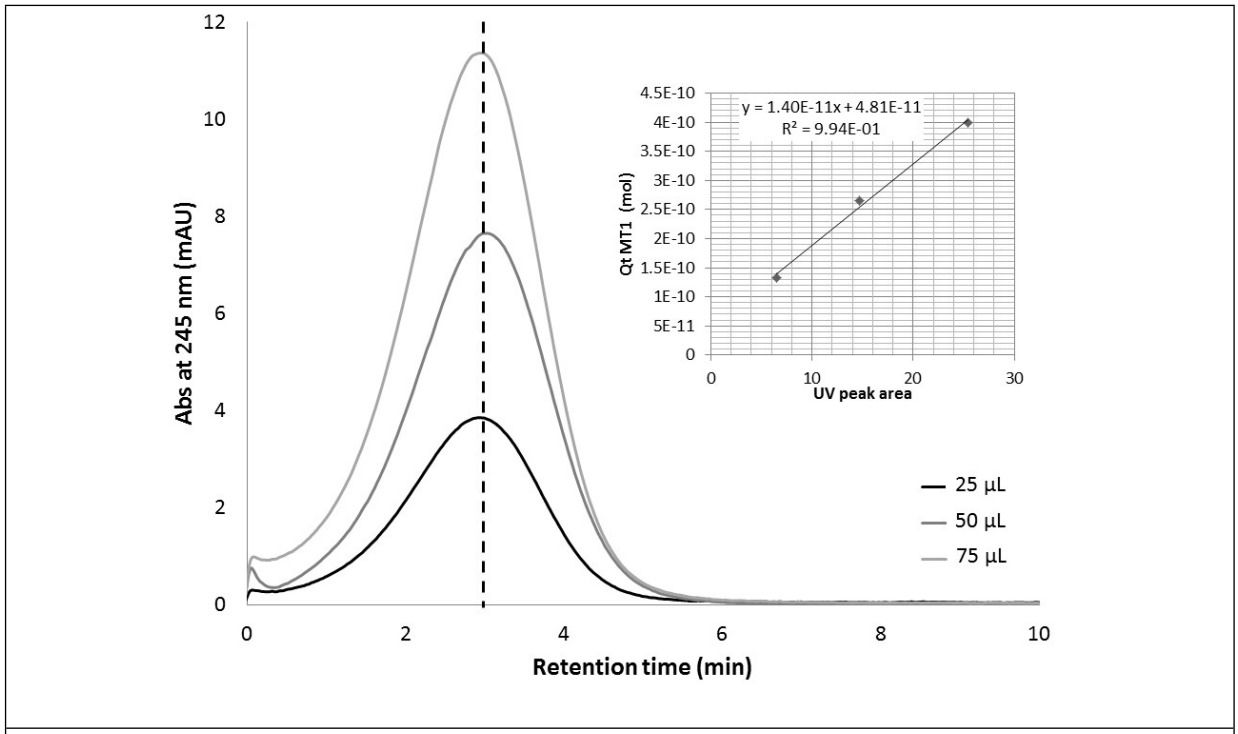

Fig. S8 Quantification of the eluted MT1. UV fractograms from absorbance at 245 nm corresponding to consecutive injections (V_{inj} = 25, 50 and 75 µL) of a 5.32 µM MT1 sample. Inset: calibration curve used for protein recovery estimation (490 µm spacer, regenerated cellulose membrane, 1 kDa cut-off, XF = 1.5 mL min^{-1}, 10 mM HEPES pH 7.1 as mobile phase). Dashed line indicated the retention time of MT1 under these conditions t_r = 2.69 ± 0.05 min.

The stoichiometry of the metal bound to MT1 can be evaluated on a mol/mol basis by a integration of the eluted peaks, first from the metal content (Zn, Cd, Ag) obtained from ICP-MS measurements, and second from the UV signal corresponding to the quantity of protein. This led to a conditional stoichiometry (Zn_2Cd_5-MT1) similar to that given by the manufacturer.

SI.3. Quantification of metal loading on MT1 following $AgNO_3$ addition

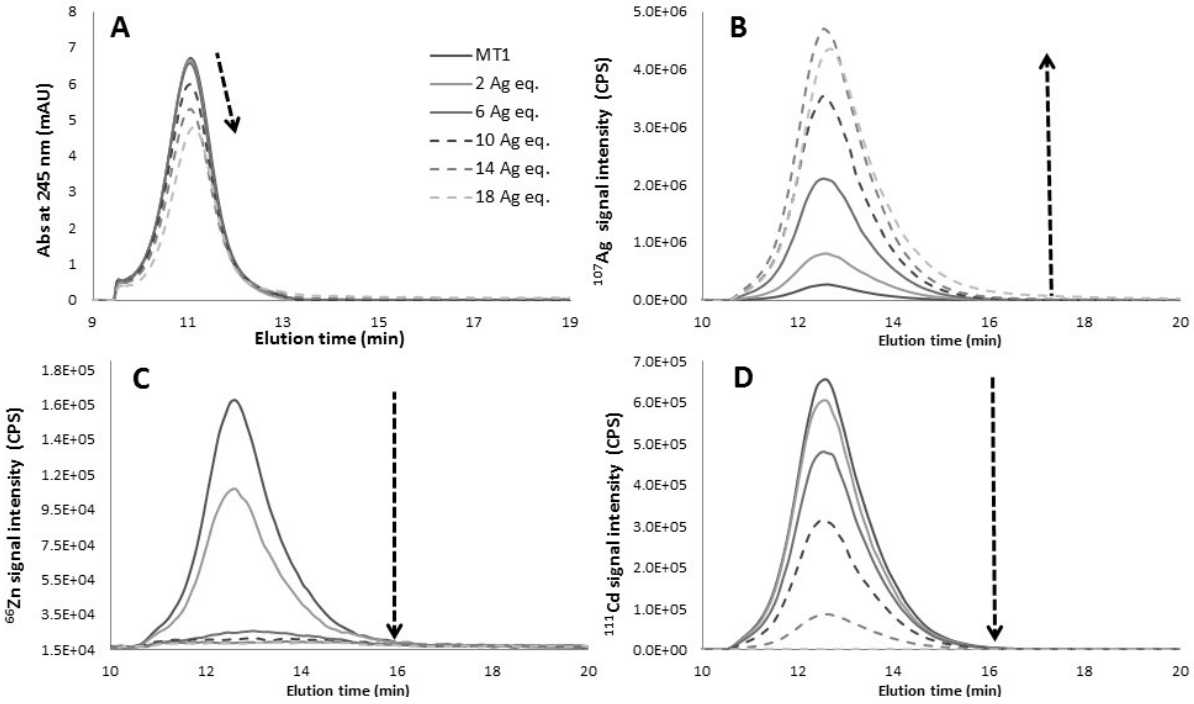

Fig. S9 Titration of MT1 by $AgNO_3$ from 2 to 18 Ag eq. (A) UV fractograms registered at 245 nm, (B) ^{107}Ag, (C) ^{66}Zn and (D) ^{111}Cd fractograms obtained by ICP-MS measurements. Silver as $AgNO_3$ was added to 200 µL of 20 µM MT1 for 1 h of contact, then the mixtures were analyzed after a 10-fold dilution in 10 mM HEPES-citrate pH 7.4. (350 µm spacer; regenerated cellulose membrane, 1 kDa cut-off; XF = 2 mL min^{-1}; 10 mM HEPES pH 7.1 as mobile phase).

Up to 6 Ag eq., the UV signal of the fractograms remained unchanged (Fig. S9A), but a slight decrease in the maximum intensity occurred for ratios above 10 eq.. In agreement with previously published data, changes occurred in the electronic absorption of MT1 within the 235-360 nm zone, especially at 245 nm upon Ag addition, but contrarily to the changes observed here, the absorbance had a tendency to increase.[2] The changes observed in the UV signal of the fractograms were accompanied by a progressive increase in the Ag signal intensity up to 14 Ag eq. (Fig. S9B). But then, at 18 Ag eq., the Ag signal intensity decreased and shifted towards longer retention times. In agreement with a metal displacement scenario, the Zn signal (Fig. S9C) reached the baseline level for more than 6 Ag eq. Cd complexed by MT1 was slightly displaced until 6 Ag eq. and was progressively eliminated by the successive

Ag additions (Fig. S9D). Changes in metal loading can influence the properties of MT1 (e.g. charge, electronic absorption). Furthermore, the retention of the various species on the membrane surface can be affected, as observed for the species formed at 18 Ag eq.. Therefore, the evaluation of the recovered protein by using the 245 nm peak integration was difficult. In order to gain further information, the results were analyzed for each experiment in terms of metal to protein ratio, either by taking into account the signal recovered at 245 nm or from the initial MT1 channel recovery (R %) without Ag (Fig. S10).

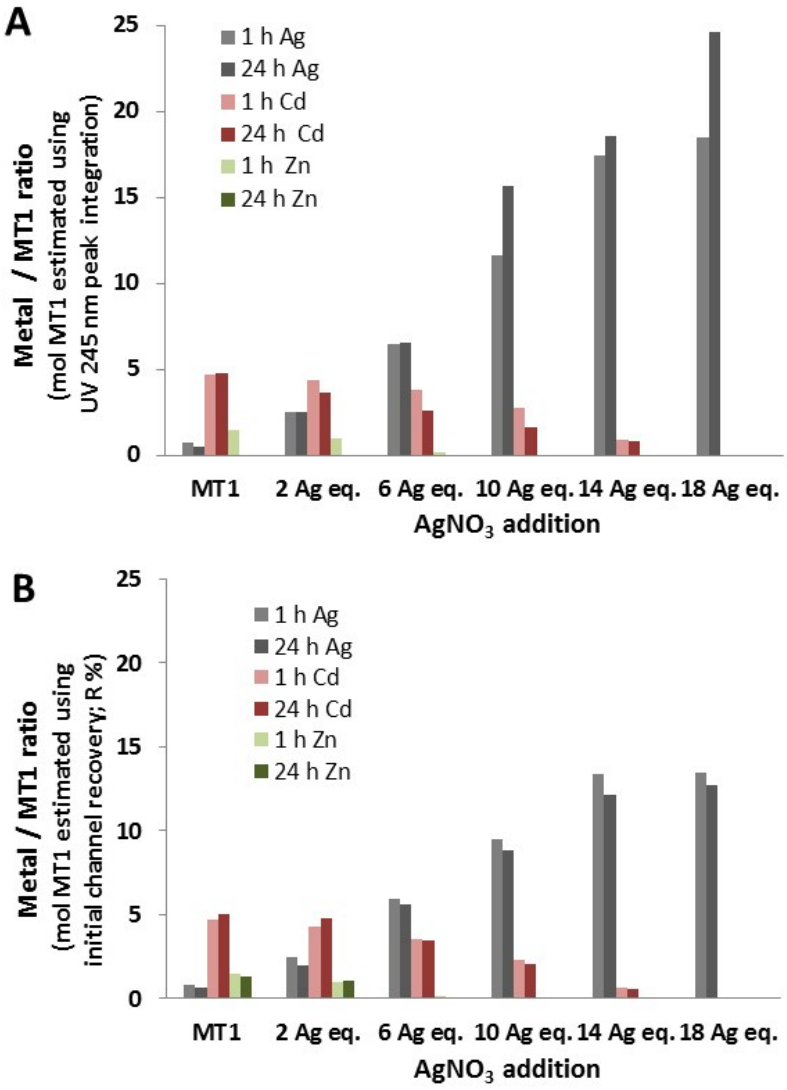

Fig. S10 Comparison between metal / MT1 ratio estimated using either the 245 nm signal integration to quantify MT1 (A) or the initial MT1 channel recovery (R %) (B) for the fractograms obtained in Fig. S9 and those obtained after 24 h of incubation (data not shown).

When the 245 nm peak integration was used to evaluate MT1 concentration, the conditional stoichiometry gave rise to unreliable results while comparing data obtained at 1 and 24 h incubations. For high Ag eq., the Ag contents obtained after 24 h incubation were largely overestimated, leading for example to a conditional stoichiometry of Ag_{24}-MT1 for 18 Ag eq. (Fig. S10A). This underlines that the protein amount was underestimated when UVD was used as a quantifier and that the absorbance at 245 nm was unstable over the 24 h incubation period and depended on the amount of Ag loaded. Alternatively, by using the initial channel recovery to estimate the protein amounts, reliable results were obtained for 1 and 24 h incubations (Fig. S10B), a result consistent with the quantities of silver added. For example, when 6 $AgNO_3$ eq. were added, the conditional stoichiometry of MT1 was $Zn_0Cd_{3.5}Ag_{5.8}$-MT1. This methodology was thus selected even if it underpinned that the MT1 concentration should stay constant over the time of experiment. This assumption could however not be valid for the 14 eq. addition or for higher ratios since the conditional speciation obtained were far below those attempted in terms of Ag-MT1 contents (e.g. $Zn_0Cd_{0.6}Ag_{12.7}$-MT1 at 14 Ag eq. and $Zn_0Cd_0Ag_{13}$-MT1 at 18 Ag eq.). Recent data obtained using capillary zone electrophoresis linked to electrospray ionization mass spectroscopy clearly show the formation of Ag_{xx}-MT1 species with loading above 13 Ag / MT.[2] Under the conditions used in this present work, it appeared that such species could not be eluted. Therefore, 11.0 ± 0.5 Ag eq. were selected to compare the interaction kinetics of AgNPs or $AgNO_3$ with MT1 (see main text).

SI.4. Optimization of the elution conditions for AgNP-Cp

In this study, special attention was paid first on using the best conditions enabling the separation of Cp from the nanoparticles (see main text) and second on evaluating eluted Cp recovery. The best separation conditions were obtained using an exponential cross-flow decay from XF = 2 to 0 mL min^{-1} over 20 min (350 µm spacer and regenerated cellulose membrane,

10 kDa cut-off). The highest Cp recovery was obtained using 10 mM HEPES pH 7.1 (as compared to 1 mM HEPES pH 7.1). This pre-optimization was carried out by comparing the recovered absorbance at 280 nm under these fractionation conditions to those obtained in the absence of cross-flow (direct injection in the channel, InjF = 0.2 mL min^{-1}, XF = 0 mL min^{-1}, DF = 1 mL min^{-1} over 15 min). These results were also compared to direct injection of the samples in a 3 ways connector replacing the AF4 channel. The fractograms obtained using both the absorbance at 280 nm and the ^{63}Cu signal were analyzed to estimate the protein recovery and the initial copper content in the proteins (Fig. S11).

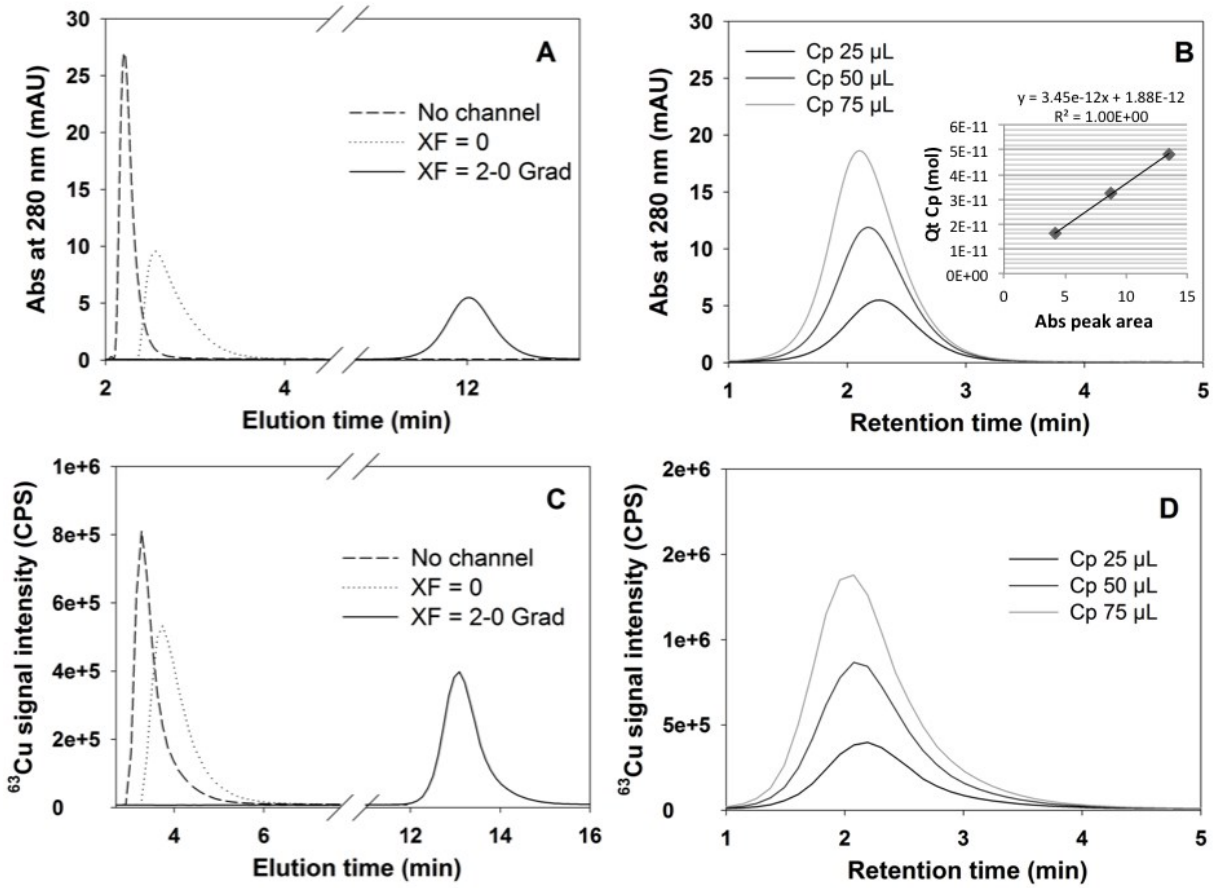

Fig. S11 Ceruloplasmin UVD fractogram at 280 nm (A, B) and ICP-MS ^{63}Cu (C, D). (A, C) Fractograms used for quantitative recovery analysis accounting for channel and fractionation effect. No channel: 3 ways connector; XF = 0: Direct elution injection in the channel; XF = 2-0 Grad: Gradient exponential decay XF = 2-0 mL min^{-1} over 20 min. (B, D) Consecutive injections of a 1 µM Cp sample (V_{inj} = 25, 50 and 75 µL) using XF = 2-0 Grad optimized protocol; inset: calibration curve of recovered protein (mol) vs. 280 nm peak area. Regenerated cellulose membrane, cut-off 10 kDa with a 350 µm spacer. Mobile phase: 10 mM HEPES pH 7.1.

By using UVD signal integration (Fig. S11A), 85.5 ± 0.5 % protein recovery compared to direct injection-elution in the channel (dotted line in Fig. S11A) was estimated under these fractionation conditions (plain line, Fig. S11A), meaning that the protein loss during the injection step was minimal. In addition, a 2% loss was evaluated and attributed to protein interaction with the channel (dashed line, Fig. S11A). Consequently, the amount of protein recovered in each run could be estimated using a linear calibration curve constructed by integration of the characteristic Cp peak at $t_r = 2.17 \pm 0.06$ min retention time (Fig. S11B) and the 16% protein loss in this experiment by using the $Area = f(mol_{recovered})$ relationship as depicted in the inset.

The stability of metal binding sites can be affected in many ways during the chromatographic process: via dilution, because of the presence of ligands in the mobile phase, and also as a result of dissociation events in the PM ⇔ P+M (where P represents protein and M for metal or AgNPs) equilibria.[3,4] These depend on the k_{off} of the various sites and the number of theoretical plates in the separation process. Copper recovery was also quantified by direct integration of the peak obtained in ^{63}Cu fractograms from ICP-MS measurements (Figs. S11C-D) and by using an external calibration (Fig. S6). The results showed that the channel had little effect on the quantity of Cu recovered when 25 µL were injected. A global recovery R = 84% was estimated under the fractionation conditions in direct line with the results obtained using UVD signals.

Thereafter, the quantitative evaluation of copper content in the Cp (Cu / Cp ratio) on a mol to mol basis could be obtained using both UVD and ICP-MS results. Under fractionation conditions, a slight effect of the injected volume was observed on the Cu / Cp ratio, i.e. 4.9, 5.5 and 5.9 ratios when 25, 50 and 75 µL were injected respectively. The latest values were however within the range of error for those obtained after acidification of Cp sample without

fractionation, in agreement with a published 5.8 Cu / Cp ratio determined from anion exchange chromatography.[5] Moreover, these results validated that the native Cp contained globally 6 copper sites that are stable under AF4 fractionation conditions.

References

1. C. A. Sötebier, F. S. Bierkandt, S. Rades, N. Jakubowski, U. Panne and S. M. Weidner, *JAAS*, 2015, 30, 2214-2222.
2. O. Palacios, K. Polec-Pawlak, R. Lobinski, M. Capdevila and P. Gonzalez-Duarte, *J. Biol. Inorg. Chem.*, 2003, 8, 831-842.
3. A. Hagège, T. N. S. Huynh and M. Hébrant, *TrAC*, 2015, 64, 64-74.
4. J. Ashby, S. Pan and W. Zhong, *ACS Appl. Mater.,* 2014, 6, 15412-15419.
5. G. Musci, T. Z. L. Fraterrigo, L. Calabrese and D. R. McMillin, *J. Biol. Inorg. Chem.*, 1999, 4, 441-446.